AUTOMATIC EXTRACTION OF FEMUR CONTOURS FROM CALIBRATED X-RAY IMAGES: A BAYESIAN INFERENCE APPROACH

Xiao Dong and Guoyan Zheng

MEM Research Center, University of Bern
Stauffacherstrasse 78, CH-3014, Bern, Switzerland

ABSTRACT

Automatic identification and extraction of bone contours from x-ray images is an essential first step task for further medical image analysis. This paper proposed a 3D statistical model based framework for the proximal femur bone contour extraction from calibrated x-ray images. The initialization to align the statistical model is solved by a particle filter on a dynamic Bayesian network to fit a multiple component geometrical model to the x-ray images. The contour extraction is accomplished by a non-rigid 2D/3D registration between the 3D statistical model and the x-ray images, in which bone contours are extracted by a graphical model based Bayesian inference. Experiments on clinical data set verified its robustness against occlusion.

Index Terms— Contour extraction, registered x-ray, statistical model, Bayesian inference, graphical model

1. MOTIVATION

Accurate extraction of bone contours from x-ray images is an important component for computer analysis of medical images for diagnosis[1][2][3], planning or 3D reconstruction of anatomic structures[4][5][6]. X-ray images may vary a lot in brightness and contrast as well as in the imaged region of anatomy. Therefore conventional segmentation techniques[1] can not offer a satisfactory solution and model based segmentation is usually implemented to obtain robust and accurate results[3][4][7][8].

In [3][8][9][10], 2D statistical models (ASM or ASM) are constructed from a training image set under the assumption that the images are taken from a certain view direction. 2D statistical models can encode both the shape and image intensity information learnt from training data set, which is helpful to improve the robustness and accuracy with noisy images. Due to the limited convergence region, 2D statistical model asks for a proper initialization. Fully automatic initialization can be accomplished by the generalized Hough transformation[8], neural nets or evolutionary algorithms[9][10]. But both the initialization and segmentation performance rely on whether the view direction assumption can be fulfilled. 3D statistical models are also used for 2D segmentation and 3D reconstruction from calibrated 2D x-ray images[4][5][6]. 3D statistical models usually only contain shape information but not the intensity information on the 2D images. But it can be used for segmenting an image taken from an arbitrary view direction. The initialization of the 3D model is usually manually defined[4][5]. Due to the dense mesh of the 3D statistical model, fully automated solutions based on evolutionary algorithm is computational expensive[11].

Bayesian network based approach[13][14][15] has been used to identify or track objects. The Bayesian network embeds the object information in a graphical model, where the constraints among subparts of the object are represented as *potentials* among nodes and the local image information correspondent to each subpart as the *observation* of each node. Bayesian network is also exploited to find deformable shapes[16][17].

We propose a 3D statistical model based fully automatic proximal femur bone contour segmentation for calibrated x-ray images, where graphical models based Bayesian inference play a key role in both the initialization to align the 3D statistical model with the x-ray images and the following up contour extraction by a non-rigid 2D/3D registration between the 3D statistical model and the 2D images.

2. METHODS

2.1. Image acquisition

In our work calibrated x-ray images from C-arm are used. Due to the limited imaging volume of C-arm, we ask for four images for the proximal femur from different view directions, of which two images focus on the proximal femoral head and the other two focus on the femoral shaft. The calibrated x-ray image set is represented by $\mathbf{I}$.

2.2. 3D statistical model of the proximal femur

A *Principal Component Analysis* (PCA) based 3D statistical model $\mathcal{M}$ with 4098 vertices of the proximal femur is con-

This project is partially supported by Swiss NCCR CO-ME.

structed from a collection of 13 CT data of the proximal femur as shown in Fig. 1(a). An instance generated from the statistical model with parameter set $\mathbf{Q} = \{\alpha, \beta_0, \beta_1, \ldots, \beta_{11}\}$ can be described as

$$\mathcal{M} : \mathbf{S}(\mathbf{Q}) = \alpha(\mathbf{S}_0 + \sum_{i=0}^{11} \beta_i \lambda_i^{\frac{1}{2}} \mathbf{P}_i) \quad (1)$$

where $\mathbf{S}_0$ is the mean model, α is the scaling factor, λ_i and $\mathbf{P}_i$ are the *i*th eigenvalue and the the correspondent eigenvector of the correlation matrix of the training data set.

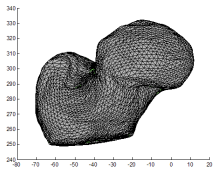

(a) PCA based 3D statistical model

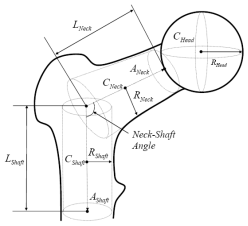

(b) Multiple component geometrical model

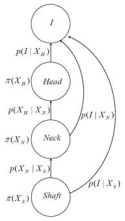

(c) The Bayesian network for the multiple component geometrical model

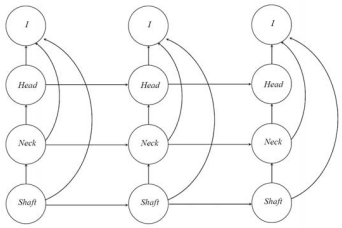

(d) The dynamic Bayesian network for fitting the multiple component geometrical model to x-ray images

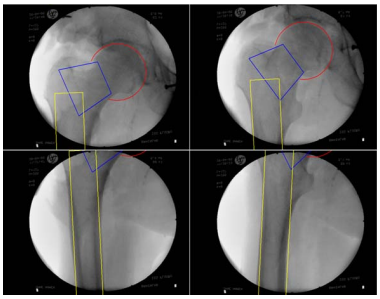

(e) Fitting the geometrical 3D model with x-ray images

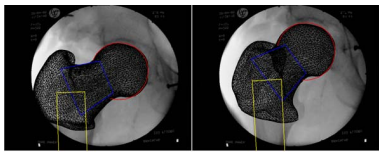

(f) Fitting the statistical model with the geometrical model

Fig. 1. Automatic initialization of the 3D statistical model

2.3. Automated initialization of the 3D statistical model

To find the initial rigid transformation $\mathbf{T}_0$ and parameter set $\mathbf{Q}_0$ to align a model instance $\mathbf{S}(\mathbf{Q}_0)$ with the observed x-ray images, we model the proximal femur by a multiple component geometrical model consisting of three components: head, neck and shaft, which are described by a sphere, a trunked cone and a cylinder with parameter set $\mathbf{X}_{geo} = \{\mathbf{X}_H, \mathbf{X}_N, \mathbf{X}_S\}$ respectively as shown in Fig. 1(b).

A graphical model is then constructed for the geometrical model as shown in Fig. 1(c). The constraints among components are encoded in the conditional distributions among nodes [13][15]. $\pi(X_S), \pi(X_N), \pi(X_H)$ are the prior information for the shaft, neck and head. The conditional distributions $p(X_N|X_S), p(X_H|X_N)$ are set so that the geometrical model can represent a meaningful anatomical structure of the proximal femur. A particle filtering on a dynamic Bayesian network (see Fig. 1(d)) is implemented to find an instance of the geometrical model $\mathbf{X}_{geo}^0$ which fits the x-ray images as shown in Fig. 1(e).

From the mean shape of the 3D statistical model $\mathbf{S}_0$, the femoral head center and radius, axes of femoral neck and shaft can be determined in the model coordinate space. The initial rigid transformation $\mathbf{T}_0$ and parameter set $\mathbf{Q}_0 = \{\alpha_0, 0, \ldots, 0\}$ can then be computed to fit the statistical model(the scaled mean shape) to the geometrical model as shown in Fig. 1(f).

2.4. 3D statistical model based contour extraction

After the statistical model initialization, the contour extraction is accomplished by a joint registration and segmentation as summarized in Algorithm 1.

2.4.1. 2D template based segmentation using belief propagation

From the silhouette of the projected 3D statistical model, we sample M points(nodes) tracing along the contour as the shape prior. Each point is described by a parameter set $\mathbf{q}_i = \{\mathbf{x}_i, \mathbf{g}_i, flag_i\}, i = 1, \ldots, M$, where $\mathbf{x}_i = (x_i, y_i)$ is the position of *i*th point in the image coordinate system, $\mathbf{g}_i = (g_{xi}, g_{yi})$ is the gradient vector of the x-ray image,$flag_i = 1$ if the current node belongs to the femur head projection silhouette and $flag_i = 0$ otherwise. The configuration of our model can then be written as $\mathbf{Q}_{model} = \{\mathbf{q}_i\}_{i=1,\ldots,M}$, where $\mathbf{g}_i$ is set as the tangent vector of the template curve at position $\mathbf{x}_i$. The configuration of a candidate contour can be written as $\mathbf{Q}_{cand} = \{\mathbf{q}_i^{'}\}_{i=1,\ldots,M}$.

We then establish a partially connected graph with M vertices as: $\mathbf{G}(\mathbf{V}, \mathbf{E}), \mathbf{V} = \{v_i, \}_{i=1,\ldots,M}, \mathbf{E} = \{e_{ij}\}_{i,j=1,\ldots,M}$,where $e_{ij} = 1$ for $(a)(|i-j| <= N_{Shaft}) \cap (i \neq j) \cap (flag_i = 0) \cap (flag_j = 0), (b)(flag_i = 0) \cap (flag_j = 1), (c)(|i - j| <= N_{Head}) \cap (flag_i = 1) \cap (flag_j = 1)$ as shown in

Fig. 2(a). N_{Head} and N_{Shaft} determine the number of connected neighbors for the head nodes and the non-head nodes respectively. Larger H_{Head} and N_{Shaft} will keep the rigidity of the shape but will fail to track deviation from the template. The reason that all the head nodes are connected with the non-head nodes is that we need the non-head nodes(which are supposed to be relatively easier to be located than the head nodes) to guide the localization of the head nodes. The correspondent factor graph is shown in Fig. 2(b).

Given the template $\mathbf{Q}_{model} = \{\mathbf{q}_i\}_{i=1,\ldots,M}$, the joint probability distribution of the factor graph with an candidate configuration $\mathbf{Q}_{cand} = \{\mathbf{q}_i^{'}\}_{i=1,\ldots,M}$ is then given by

$$p(\mathbf{Q}_{cand}) = \frac{1}{Z}\prod_i \psi_i(\mathbf{q}_i^{'}) \prod_{e_{ij}=1} \psi_{ij}(\mathbf{q}_i^{'}, \mathbf{q}_j^{'}) \qquad (2)$$

where $\psi(\mathbf{q}_i^{'}) = dot(\mathbf{g}_i, \mathbf{g}_i^{'})$,which means to penalize candidates with weak gradient amplitude and inconsistent gradient direction with the model.

$\psi(\mathbf{q}_i^{'}, \mathbf{q}_j^{'}) = e^{-(\mu \frac{(\mathbf{x}_i^{'}-\mathbf{x}_j^{'})\cdot(\mathbf{x}_i-\mathbf{x}_j)}{\|\mathbf{x}_i^{'}-\mathbf{x}_j^{'}\|\|\mathbf{x}_i-\mathbf{x}_j\|} + \nu \frac{\|\|\mathbf{x}_i^{'}-\mathbf{x}_j^{'}\|-\|\mathbf{x}_i-\mathbf{x}_j\|\|}{\|\mathbf{x}_i-\mathbf{x}_j\|})}$, which is set so that the global shape of the model will be kept by penalizing the deviation of the angle and distance between vertices from our model.

---

1. *Simulated x-ray and silhouette extraction*
Given the current instanced statistical model $\mathcal{M} : \mathbf{S}(\mathbf{Q}^n)$ and the transformation $\mathbf{T}^n$, project the aligned statistical model on each of the K x-ray image planes using the projection geometry of each x-ray image. From the simulated x-ray images the silhouettes $\{\mathbf{C}_{model}^{k,n}\}_{k=0,\ldots,K-1}$ are extracted[5].
2. *2D template based segmentation*
On each x-ray image, taking the correspondent silhouette of the projected statistical model $\mathbf{C}_{model}^{k,n}$ as a template, a graphical model based shape matching is implemented to search for the bone contour $\mathbf{C}_{image}^{k,n}$ as a Bayesian inference task.
3. *Nonrigid 2D/3D registration*
A 2D/3D nonrigid registration is carried out to fit the extracted bone contours $\{\mathbf{C}_{image}^{k,n}\}_{k=0,\ldots,K-1}$ and the statistical model $\mathcal{M}$, which results in an updated model instance $\mathcal{M} : \mathbf{S}(\mathbf{Q}^{n+1})$ and rigid transformation $\mathbf{T}^{n+1}$
4. Go to 1, until the procedure converges.

Algorithm 1. 3D statistical model based contour segmentation

Under these definitions, a bone contour that keeps the global shape of our model and at the same time locates itself to the strong edge positions can be obtained by a *Maximal Likelihood*(ML) estimation as

$$C_{image}^{*} = \max_{\mathbf{Q}_{cand}=\{\mathbf{q}_i^{'}\}} \prod_i \psi_i(\mathbf{q}_i^{'}) \prod_{e_{ij}=1} \psi_{ij}(\mathbf{q}_i^{'}, \mathbf{q}_j^{'}) \qquad (3)$$

In our approach, the candidate positions for each node of the bone contour are sampled along the normal direction of the model and standard loopy belief propagation[16] is used to approximate the ML estimation as shown in Fig. 3(a).

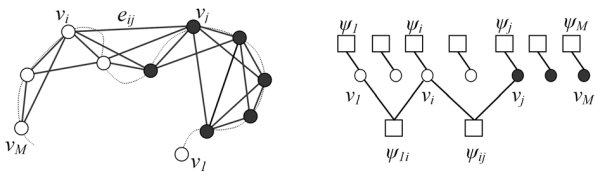

(a) Graphical model for the contour extraction, filled dots: head nodes, circles: non-head nodes

(b) Factor graph for the graphical model for the contour extraction

Fig. 2. The Bayesian network for contour extraction

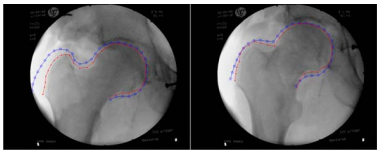

(a) Graphical model based 2D segmentation, where circles show the projected silhouettes and dots show the extracted contours

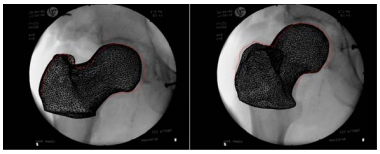

(b) 2D/3D nonrigid registration to fit the 3D statistical model to the extracted bone contours

Fig. 3. Contour extraction as Bayesian inference

2.4.2. 2D/3D nonrigid registration

Our statistical model can be fitted to the extracted bone contours $\{C_{image}^{k,n}\}$ as a 2D/3D nonrigid registration procedure. For each point P_l on the extracted bone contour, the correspondence between its backprojection line $BP(P_l)$ and a vertex $v_{corr(P_l)}$ on the current instanced statistical model $\mathcal{M} : \mathbf{S}(\mathbf{Q}^n)$ and its current transformation $\mathbf{T}^n$ can be established. Project $v_{corr(P_l)}$ on $BP(P_l)$ will generate a correspondent 3D point pair $(v_{corr(P_l)}, Proj(v_{corr(P_l)}, BP(P_l)))$. A rigid transformation $\mathbf{T}_{update}^{n+1}$ can be calculated to align the current statistical model $\mathcal{M} : \mathbf{S}(\mathbf{Q}^n)$ to the extracted contours. The rigid transformation can then be updated as $\mathbf{T}^{n+1} = \mathbf{T}_{update}^{n+1}\mathbf{T}^n$. The residual error between correspondent point pairs can then be compensated by the constrained deformation of the statistical model[12]. An example of the nonrigid registration is shown in Fig. 3(b).

3. EXPERIMENTAL RESULTS

We verified our approach on two set of clinical data, each data set includes four calibrated x-ray images of the proximal femur. We first run our algorithm on the original data set with parameters set as $M = 35, N_{Head} = 4, N_{Shaft} = 3, \mu = 2, \nu = 1$ and the results are shown in Fig. 4(a) and 4(b). To further verify its performance against occlusion, we added artificial occlusion with different sizes to the x-ray images. The contour extraction results with $M = 35, N_{Head} = 5, N_{Shaft} = 6, \mu = 2, \nu = 1$ are shown in Fig.

4(c) and 4(d). It can be observed that due to the existence of occlusion, we have to select larger N_{Head} and N_{Shaft} to hold the global shape of the contour, which on the other hand leads to a failure in tracking local deviation between the real contour and the template in the femur neck area as shown in Fig. 4(c) and 4(d)

4. CONCLUSIONS

We introduced a 3D statistical model based fully automatic bone contour extraction framework from calibrated x-ray images. The automatic initialization is achieved by fitting a simplified multiple component geometrical 3D model to the observed x-ray images. The 3D model based initialization algorithm does not ask for strict view direction assumption compared with 2D model or 2D image feature based initialization. The 3D statistical model based bone contour extraction is solved as a simultaneous 2D/3D registration and segmentation. The model based segmentation is accomplished by a Bayesian inference procedure which in principle can overperform than active contour and AAM/ASM by simultaneously optimize both the global shape constraints and local image feature information. Experiments on clinical data sets verified the validity and its performance in the case of occlusion.

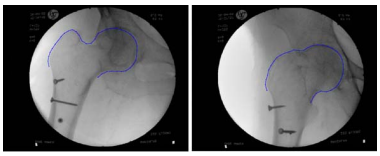

(a) Data set 1, no occlusion

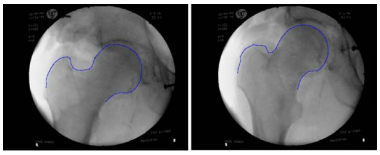

(b) Data set 2, no occlusion

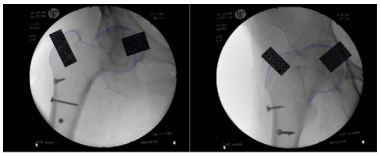

(c) Data set 1, with artificial occlusion

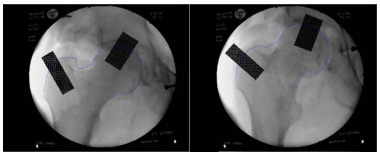

(d) Data set 2, with artificial occlusion

Fig. 4. Results of automatic proximal femur bone contour extraction on clinical data

5. REFERENCES

[1] Y. Chen, X. H. Ee, W. K. Leow, and T. S. Howe,"Automatic Extraction of Femur Contours from Hip X-ray Images," *CVBIA05*, pp. 200-209, 2005.

[2] R. de Luis-Garcia, M. Martin-Fernadez, J. I. Arribas, and C. Alberola-Lopez, "A Fully Automatic Algorithm for Contour Detection of Bones in Hand Radiographs Using Active Contours," *ICIP03*, Vol. III, pp. 421-424, 2003.

[3] M. G. Roberts, T. F. Cootes, and J. E. Adams, "Automatic Segmentation of Lumbar Vertebrae on Digitised Radiographs using Linked Active Apperance Models," *MIUA 2006*, Vol. I, pp. 120-124, 2006.

[4] S. Benameur, M. Mignotte, S. Parent, H. Labelle, W. Skalli, and J. A. de Guise "3D/2D Registration and Segmentation of Scoliotic Vertebrae Using Statistical Models," *Computerized Medical Imaging and Graphics*, Vol. 27(5), pp. 321-337, 2003.

[5] H. Lamecker, T. H. Wenckebach, H. C. Hege, "Atlas-based 3D-Shape Reconstruction from X-ray Images," *ICPR06*, Vol. I, pp. 371-374, 2006.

[6] T. S. Tang, and R. E. Ellis,"2D/3D Deformable Registration Using a Hybrid Atlas," *MICCAI 2005*, Vol. 3750, pp. 223-230, 2006.

[7] G. Behiels, D. Van der Meulen, F. Maes, P. Suetens, and P. Dewaele, "Active Shape Model-based Segmentation of Digital X-ray Images," *MICCAI*, pp. 128-137, 1999.

[8] B. Howe, A. Gururajan, and L. R. Long, "Hierarchical Segmentation of Cervical and Lumbar Vertebrae Using a Customised Generalized Hough Transform and Extensions to Active Appearance Models," *Proc. IEEE 6th SSIAI*, pp. 182-186, March 2004.

[9] M. Seise, S. J. McKenna, I. W. Ricketts, and C. A. Wigderowitz,"Probabilistic Segmentation of the Knee Joint from X-ray Images," *MIUA 2006*, pp. 110-114, 2006.

[10] M. de Bruijne, M. Nielsen, "Image Segmentation by Shape Particle Filtering," *ICPR04*, Cambridge, United Kingdom, 2004.

[11] B. Ma, and R. E. Ellis, "Surface-based Registration with a Particle Filter," *MICCAI04*, pp. 566-573, 2004.

[12] K. T. Rajamani, J. Hug, L.-P. Nolte, and M. Styner, "Bone Morphing with Statistical Shape Models for Enhanced Visualization," *Proc. Midical Imaging 2004*, pp. 122-130, 2004.

[13] M. W. Lee, and I. Cohen, "Human Upper Body Pose Estimation in Static Images," *ECCV04*, LNCS 3022, pp. 126-138, 2004.

[14] L. Sigal, S. Bhatia, S. Roth, M. J. Black, and M. Isard, "Tracking loose-limbed people," *Proc. Computer Vision and Pattern Recognition*, vol. 1, pp. 421-428, 2004.

[15] Y. Wu, G. Hua and T. Yu, "Tracking articulated body by dynamic Markov network", Proceeding of IEEE International Conference on Computer Vision, Nice, France, 2003.

[16] J. Coughlan, S. Ferreira, "Finding deformable shapes using loopy belief propagation," *ECCV02*, pp. 453-468, 2002.

[17] A. Rangarajan, J. Coughlan, and A. L. Yuille, "A Bayesian Network Framework for Relational Shape Matching," *ICCV03*, pp. 671-678, 2003.